

Recording Extracellular Activity in the Developing Cerebellum of Behaving Rats

Greta Sokoloff and Mark S. Blumberg

Abstract

The *in vivo* extracellular activity of the cerebellum has been intensively investigated in adult animals to understand its roles in learning and memory and sensorimotor integration. Here we describe a method for studying extracellular activity in the cerebellum of unanesthetized, behaving infant rodents over the first 2 postnatal weeks, a time of substantial cerebellar circuit development. The study of extracellular activity during cerebellar development in behaving infants provides a unique opportunity to relate neural activity not only to cerebellar circuit development but to behavioral development as well. We propose that studying extracellular neural activity in the developing cerebellum provides a model system for examining the complex interactions between behavior and neural activity and how they contribute together to functional neural circuit development.

Key words Cerebellum, Sleep, Twitching, Infant rodent, Methods, Neural recording

1 Introduction

Beginning with the first identification of the Purkinje cell in 1837, the cerebellum has fascinated neuroanatomists [1]. For developmental neurobiologists, the protracted postnatal development of the cerebellum in mammals, especially rodents, has spurred recent interest in a broad range of research questions addressing Purkinje cell development, synapse formation and elimination, cerebellar circuit formation, and motor learning [2–8].

Figure 1 presents representative coronal sections through the cerebellar cortex at postnatal day (P) 4, P8, and P12. It is readily apparent that there is a dramatic increase in size alone over this single week. Figure 1 also presents a subset of the cerebellar milestones that occur during the first 2 postnatal weeks in rats. At birth, Purkinje cells are immature with short dendritic processes and are not yet organized into a single Purkinje cell layer [3, 7]. Also at birth, mossy fibers form transient direct connections with Purkinje cells and innervate cells of the cerebellar nuclei (CN) [9–11]. In the first few

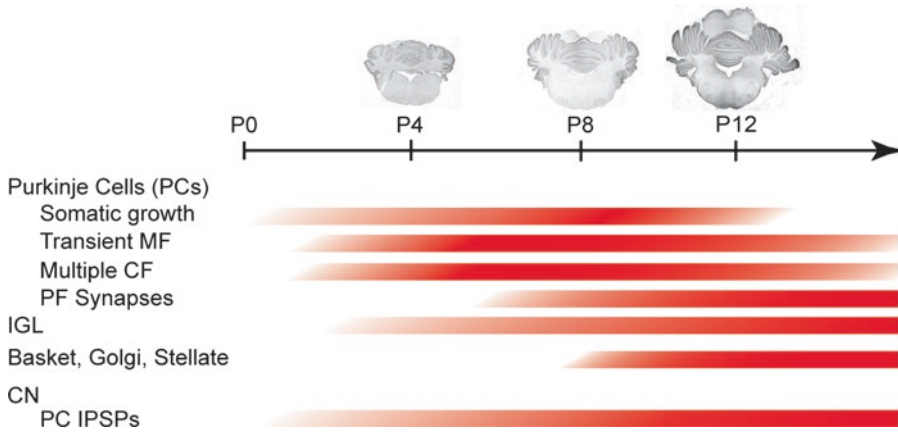


Fig. 1 A timeline illustrating some of the major developmental events in the cerebellum during the first 2 postnatal weeks. *Top*, Nissl-stained, coronal sections of the cerebellum and brainstem in P4, P8, and P12 rats. *Bottom*, timeline based on anatomical and electrophysiological studies depicting earliest observation, peak, and end (if occurring by P16) of each event. Abbreviations: *PC* Purkinje cell, *MF* mossy fiber, *CF* climbing fiber, *PF* parallel fiber, *IGL* internal granular layer, *IPSP* inhibitory postsynaptic potential

days after birth, climbing fiber innervation of Purkinje cells increases, and multiple climbing fibers innervate each Purkinje cell [8, 12–14]. Around the same time, granule cells begin to proliferate in the external granular layer (EGL) and begin their migration to the internal granular layer (IGL) [1, 2, 4].

During the second postnatal week, the Purkinje cell soma reaches its adult size, and the synapses of extraneous climbing fibers are weakened as the “winner” begins to translocate along the apical dendrite of the Purkinje cell [6, 7]. As granule cells migrate, they form connections with mossy fibers, and the transient mossy fiber connections on the Purkinje cell soma diminish as parallel fiber synapses begin to form, connecting mossy fibers to Purkinje cells via granule cells [2–4, 8, 11, 15]. Also during the second postnatal week, basket, Golgi, and stellate cells become functional [3, 8]. So, for the 2-week-old rat, the majority of the cerebellar circuit is established, although there is continued cell migration and dendritic growth and refinement through the third postnatal week and into adulthood [2–4, 7, 16].

Importantly, despite this protracted cerebellar development in rats, the Purkinje cells, neurons in the deep cerebellar nuclei (CN), as well as the primary input pathways—climbing and mossy fibers—are already functioning within the first few postnatal days [8, 10, 12, 16–19]. Specifically, climbing fibers and mossy fibers transmit sensory information from both the periphery and cerebral cortex to Purkinje cells and CN neurons by P3 [10, 17, 18]. Also, Purkinje cells at this time are able to produce inhibitory postsynaptic potentials (IPSPs) on CN neurons [10].

Molecular cues play an important role in early cerebellar development [15, 20, 21], as do activity-dependent mechanisms [22]. For example, activated climbing fibers facilitate synapse elimination and, ultimately, climbing fiber translocation at Purkinje cells [23–27]. However, it is not yet known how different sources of neural activity drive activity-dependent development of the infant cerebellum [22]. Therefore, the study of extracellular activity in the developing cerebellum is crucial for understanding the role of both spontaneous and evoked activities on cerebellar circuit formation and synapse elimination.

Due to its protracted development, the cerebellum is more susceptible than many other brain regions to perturbations that disrupt activity-dependent processes necessary for cerebellar development and connectivity with forebrain areas [28]. Importantly, the early, seminal studies of extracellular cerebellar activity were performed using anesthetized infant rats. Among its many drawbacks, anesthesia lowers the firing rates of Purkinje cells [29]. Thus, the best approach to understanding cerebellar activity and functionality in early development is to use unanesthetized subjects, thereby providing direct access to patterns of spontaneous and evoked neural activity across a period of rapid developmental change. Significantly, a better understanding of the role of neural activity on activity-dependent developmental processes may illuminate the contributions of cerebellar dysfunction to the etiology of neurodevelopmental disorders such as autism and schizophrenia [28, 30, 31].

2 Methods: Extracellular Cerebellar Neural Activity and Behavior in Infant Rodents

2.1 Head-Fix Method for Neural Recording in Behaving Infant Rodents

Using the head-fix method described below, it is possible to record from P1 to P12 in rats and from P4 to P15 in mice. Pups can be tested at younger and older ages with appropriate modifications to the apparatus and method. The reader should refer to our previously published primer which contains a comprehensive list of studies that have used this and similar methods to record extracellular activity in numerous brain regions in infant rodents [32]. Here we detail our head-fix method with special consideration for the cerebellum.

2.2 Constructing a Head-Fix

The head-fix is constructed using a metal washer, two strips of metal, hex nuts, locking washers, and machine screws. Inner and outer diameters of the washer are determined by the age (i.e., size and/or weight) of the subject and the brain area to be recorded from. For illustration purposes, Fig. 2 shows a washer size that is appropriate for week-old rats. Once all the materials are organized, the two metal strips are bent at 90° and glued (Loctite© Liquid

Super Glue, Henkel Corporation, Rocky Hill CT) or welded to opposite sides of the washer. Machine screws are inserted through holes drilled into the bent ends; the metal strips and nuts are screwed in place over locking washers. (Regular washers will work but will need to be tightened with each use.) To add stability, liquid Super Glue may be applied over the nuts and screws, but with a functioning locking washer, this should not be necessary.

Machine screws are sized to fit into the ends of ear bars that can be secured in a standard stereotaxic apparatus. Washer and metal strip thicknesses determine the rigidity of the head-fix. With older pups, a more rigid head-fix helps to minimize, or negate, movement artifact in the extracellular recording. For recordings with infant mice, the device can be fashioned from thinner metal components or even firm plastic with little loss of stability.

For extracellular recordings in the cerebellum, the head-fix is improved with modifications to the inner portion of the metal washer. Either removing a portion of the caudal part of the washer or drilling out part of the inner diameter will provide a window that is open to the occipital ridge, thereby facilitating access to the area of interest; see the inset in Fig. 2 for examples of modifications that can be made for small infant rodents (lower right) or cerebellum and hindbrain recording (upper left). Importantly, each head-fix costs less than \$3.00 and is easily cleaned and repaired for reuse.

2.3 Equipment and Apparatus

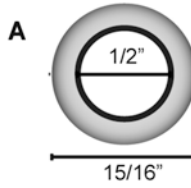
Our setup for stereotaxic extracellular recording is shown in Fig. 3. A standard stereotaxic apparatus is housed within a Faraday cage atop a sturdy table. All electrical equipment within the cage are grounded. The thermal environment is controlled using a small double-walled glass chamber (constructed in a glass blowing lab) that is placed directly under the head-fixed pup. Before testing, a water circulator is turned on, and hot water is circulated through the chamber to warm the ambient environment. In the absence of having a glass blower at your institution, the Heated Hard Pad (Braintree Scientific, Braintree, MA) can be used or, alternatively, a low-noise electrical heated mat.

2.4 Surgery

On the day of testing, a pup is removed from the home cage. It is important to select a pup with a large milk band and within the appropriate weight range for its age. Using these selection criteria, you more reliably ensure overall health and adequate nutrition and hydration for the experimental session. If the duration of the experiment is expected to be long, pups can be intubated with commercial half-and-half or milk formula (3% of body weight in mL). Intubation should be done before placing the pup in the stereotaxic apparatus. We find that, without intubation, week-old rats maintain normal body temperatures and exhibit normal sleep-wake cycles following separation from the dam for up to 8 h [33].

Constructing a head-fix

Metal washer
Stainless steel
Thickness: 0.03-0.07"



Metal sheet
Hardened stainless steel
6"X6" sheet
Thickness: 0.018"



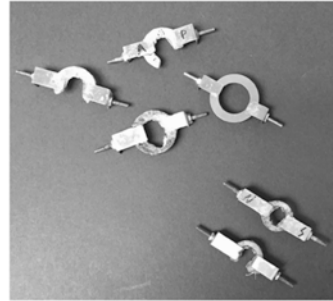
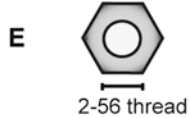
Full thread, slotted
flathead machine
screw (X2)



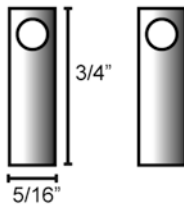
Split-lock washer
for size 0 screw (X2)



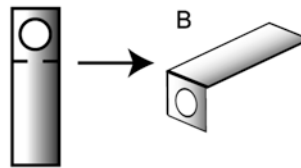
Hex nut (X2)



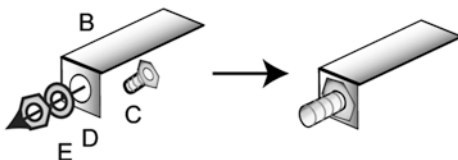
1. Cut two strips from metal sheet and drill hole in each at one end.



2. Bend each strip to a 90° angle, at the end with the hole, to create the head-fix arm.



3. Put the threaded end of the screw through the hole in the arm. Thread washer and nut onto screw and tighten.



4. Using super glue, affix arms to washer. Allow glue to cure until set.

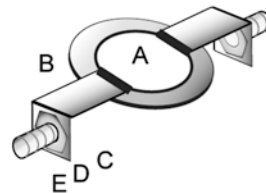


Fig. 2 Materials for building a head-fix and the subsequent steps for assembling it. *Inset*, examples of different sizes and modifications that can be used for the head-fix method in postnatal rodents. Specifications are standard, the head-fix washer size, screw length, and head-fix arm length will vary with the age of the pup and the testing environment. We purchase parts from McMaster-Carr (Elmhurst, IL), but any hardware supplier should stock these products

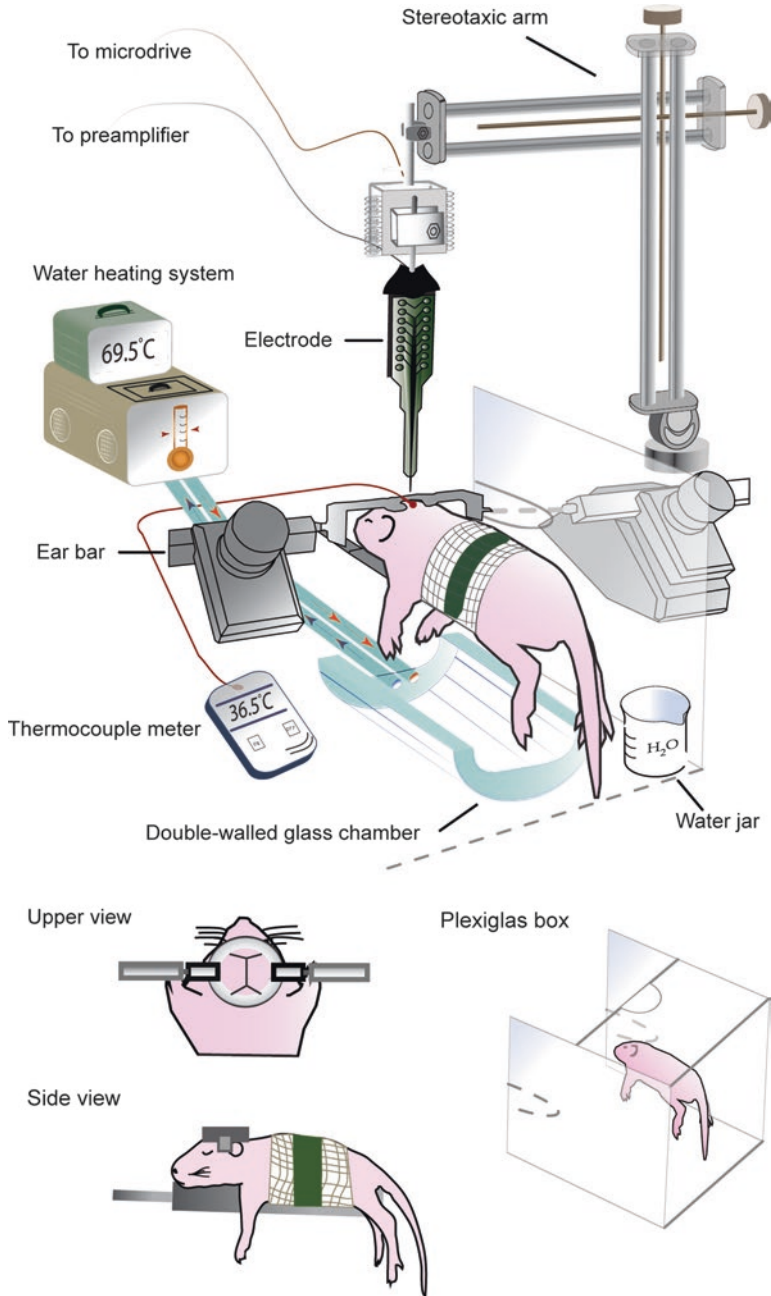


Fig. 3 An illustration of the recording setup for head-fixed infant rodents adapted from [32]. A head-fixed pup is secured to an elevated platform with tape. The head-fix attaches to ear bars that can be secured to the stereotaxic apparatus. A double-walled glass chamber is positioned under the pup so that temperature-controlled water can heat the ambient air. A Plexiglas box surrounds the pup on three sides to help maintain air temperature, and water-filled beaker inside the box helps to maintain adequate humidity. Brain temperature is monitored with a thermocouple inserted into a predrilled hole in the skull. The recording electrode is attached to a headstage and can be lowered into the cerebellum using a microdrive. Reprinted by permission of John Wiley & Sons, Inc.

Using an induction chamber filled with isoflurane (rats, 3–5%; mice, 2–3%), anesthesia is induced. Once anesthetized, the pup is placed in a prone position on a heating pad. Anesthesia is maintained with an anesthesia cone over the pup's snout. 2–3% isoflurane is typically sufficient for maintenance, but respiration should be closely monitored throughout the surgery, and pedal (foot) and pinnal (ear) reflexes should be tested regularly to insure an appropriate level of anesthesia.

To record electromyographic (EMG) activity, 27 g sterile needles are used to insert custom-made bipolar hook electrodes into the skeletal muscle (304 HPN, California Fine Wire, Grover Beach, CA). Uninsulated stainless steel wire (304, California Fine Wire) is looped transdermally on the back of the pup. EMG and ground wires are secured to the skin at insertion points with collodion. A 2" × 2" gauze pad is unfolded and wrapped around the pup's torso and secured with tape (e.g., 3M Micropore, St Paul, MN). The gauze is trimmed to the appropriate length to ensure that the hind limbs are well outside the wrap.

To prepare the skull for electrode implantation, the skin overlying the skull is removed using surgical scissors or a scalpel. The exposed skull is cleaned of connective tissue and dried using bleach or hydrogen peroxide. Bupivacaine is applied topically to scalp incisions to minimize pain. Loctite® Super Glue Gel Control (Henkel Corporation) is applied to the metal washer at least 15 min before it is fixed to the skull; when applied to the skull, the glue should be tacky. Before attaching the head-fix to the skull, Vetbond (3M) can be applied beneath the surface of the skin around the incision to glue it back and away from the skull, which helps ensure a secure attachment of the head-fix. Make sure to align the head-fix over the skull before positioning it so that the midline of the skull is aligned at the middle of the head-fix. Place the head-fix onto the exposed skull and apply light pressure for approximately 10 s. Ensure the head-fix is level on all planes and make any adjustments as needed. Once attached, liquid or gel Super Glue (Henkel Corporation) can be applied to the inner circumference of the head-fix to reinforce adhesion or fill in gaps between the head-fix and skull. For general analgesia, the pup is administered an NSAID (e.g., Rymadyl; 5 mg/kg s.c.). Next, the pup is temporarily wrapped in a second layer of gauze in order to restrain movement while the head-fix sets. Finally, the pup is placed in a ventilated, humidified incubator maintained at thermoneutrality (e.g., 35 °C for a P8 rat) for approximately 1 h. The entire surgical procedure takes approximately 10–15 min.

After 1 h in the incubator, the head-fix should be securely attached to the skull. At this point, for drilling holes in the skull, the pup is moved to a stereotaxic apparatus outfitted with an adaptor and anesthesia mask (Mouse and Neonatal Rat Adaptor and Gas Anesthesia Mask; Stoelting, Wood Dale, IL). The threaded end of the screws on the head-fix fits into the ear bar holders on the adaptor.

Table 1
Stereotaxic coordinates for extracellular cerebellar recordings in infant rats and mice

Age and species	AP (mm from lambda)	ML (mm)	DV (mm)	Angle (R → C)
<i>Cerebellar cortex</i>				
P3-P4 rat	-1.0 to -2.0	± 1.3 to 2.0	-1.2 to -3.4	8–10°
P6 rat	-1.0 to -1.5	± 1.5 to 2.0	-1.3 to -3.7	10–12°
P7-P9 rat	-1.1 to -2.4	± 1.7 to 2.0	-1.2 to -3.8	8–10°
P8-P9 mouse	-1.0 to -2.6	± 1.0 to 1.9	-1.0 to -2.3	10–14°
P11-P12 rat	-2.0 to -3.3	± 1.7 to 2.1	-1.7 to -3.1	10–12°
P14-P15 mouse	-1.1 to -2.5	± 1.1 to 1.4	-1.0 to -1.7	10–14°
<i>Interpositus nucleus</i>				
P7-P9 rat	-2.5 to -2.9	±2.0	-3.2 to -3.8	10–12°
P11-P13 rat	-3.7	±2.0	-3.5 to -4.5	None

AP anterior/posterior, ML mediolateral, DV dorsoventral, R rostral, C caudal, L lateral, M medial

Under light isoflurane anesthesia, stereotaxic coordinates are used to drill holes for recording electrode placement, ground and reference wires, and a thermocouple. Also at this time, cannulae can be inserted and secured to the skull for pharmacological manipulations, and/or brain lesions can be produced. Table 1 provides a list of coordinates we have used to record from cerebellar cortex and interpositus nucleus in rats and mice during the first 2 postnatal weeks.

When the pup is ready, the second layer of gauze is removed so the limbs are free to move. The pup is moved to the recording chamber and set on a narrow support platform that is attached to a metal rod that fits into the nosepiece holder of the stereotaxic apparatus. The pup is secured to the platform by wrapping a piece of tape around the pup and the platform. The nosepiece holder can be adjusted for height, and the angle can be adjusted to ensure comfortable positioning between the pup's head and body. Each ear bar is attached to the threaded end of the screws in the head-fix and then secured to the stereotaxic apparatus; take this opportunity to ensure that the skull is leveled and adjusted, if necessary. When this process is complete, the pup should appear comfortable with its legs dangling on either side of the platform; when the pup moves its limbs, you should not observe any movement of the head.

Next, a Plexiglas box is placed around the pup to help control air temperature and humidity around the pup. The Plexiglas box has three walls and fits inside the arms of the stereotaxic apparatus; the side walls have slots cutout at the height of the ear bars to allow the box to surround the pup. A separate piece of Plexiglas is used to cover the top of the box (this piece can be made to accommo-

date the electrode holder). The addition of a small, open jar of water placed within the box helps to humidify the air.

To measure brain temperature during acclimation and recording, we use a chromel-constantan thermocouple (Type E; #TT-E-40, Omega Engineering, Stamford, CT) and a thermocouple meter (450-AET, Omega Engineering). The thermocouple can be inserted anywhere in the brain but preferably distant from the recording location. For cerebellar recordings, we typically monitor brain temperature in the cerebral cortex. The thermocouple remains in the brain for the duration of the experiment, but the meter is turned off during data collection as it may cause electrical noise in the extracellular recording. For neurophysiological recordings, brain temperature should be maintained at 36–37 °C. Depending on the distance of the pup from the heated glass chamber, the water bath is set at 50–65 °C. It is important that the pup's limbs and tail cannot make contact with the heat source. If necessary, a heat lamp, located outside the Faraday cage, can be used to help maintain body and brain temperature; however, the lamp should never be aimed directly at the pup. It is important, especially with mice, that brain temperature not exceed 37 °C; finally, we have found that slow, steady rewarming is optimal for recovery and subsequent behavior.

2.5 Experimental Testing

Once the pup is in the recording chamber, wait at least 1 h. for recovery from anesthesia and attainment of a stable brain temperature. A well-acclimated pup should cycle regularly between sleep and wake, with sleep as the predominant behavioral state; we use the combination of EMG and behavioral observation to determine sleep and wake states. We find that EMG electrodes inserted into the nuchal muscle provide the most clear cycling between high and low muscle tones: A well-acclimated pup will exhibit clear periods of atonia (indicative of sleep) alternating with brief periods of high muscle tone (indicative of wake); chronic, low-amplitude muscle tone (as distinct from atonia) typically indicates that the pup needs more time to acclimate. Periods of active (or REM) sleep are characterized by myoclonic twitches of the limbs and tail that occur against a background of atonia. In contrast, periods of wakefulness are characterized by high-amplitude, coordinated wake movements (e.g., stepping movements, stretching) against a background of high muscle tone. A third behavioral state, quiet sleep, can be characterized as periods when the pup exhibits low muscle tone and behavioral quiescence. However, it should be noted that it can be difficult to distinguish between quiet wake and quiet sleep in infant rats younger than P11 because cortical slow waves (i.e., delta) do not emerge until then [33].

Once the pup is cycling regularly between sleep and wake, the experiment can begin. We use 16-channel silicon electrodes (NeuroNexus, Ann Arbor, MI), which give us well-resolved extracellular neural activity (site size: 177 μm^2 ; <http://neuronexus>).

[com/images/Impedance.pdf](#)). Before insertion of the electrode, we dip it in fluorescent DiI (Vybrant DiI Cell-Labeling Solution; Life Technologies, Grand Island, NY) for subsequent histological verification of electrode placement; of course, other electrode marking protocols will work. Using a pneumatic drum drive (FHC, Inc., Bowdoin, ME), the electrode is slowly lowered into the pre-drilled hole in the skull, and the reference/ground is inserted through a hole in a distant brain region. For cerebellar recordings, we typically insert the reference/ground electrode (Ag/AgCl, 0.25 mm diameter; Medwire, Mt. Vernon, NY) into the cerebral cortex. Once the desired depth is achieved and neural activity is observable, we allow the electrode to stabilize within the brain tissue for at least 10 min before starting data acquisition. During data acquisition, in addition to EMG and neurophysiological data, an observer scores behavior by pressing coded event keys.

The electrodes connect to a headstage that is connected to a battery-operated preamplifier inside the Faraday cage. All acquired signals are then sent to a data acquisition system (Tucker-Davis Technologies, Alachua, FL). For studies where time-locked behavioral or kinematic measures are required, a video camera can be used to capture synchronized video data. Hook electrodes for recording EMG connect to a bank of micro-grabbers, located inside the Faraday cage, that are connected to differential amplifier (A-M Systems, Sequim, WA) that amplifies (10,000 \times) and filters (300–5000 Hz bandpass) the EMG signal; a 60 Hz notch filter is also used. The neural signals are amplified (10,000 \times) and filtered for multiunit activity (500–5000 Hz bandpass) or, alternatively, not filtered to allow for subsequent analysis of both unit activity and LFP. Neural and EMG signals are sampled at 25 and 1 kHz, respectively.

2.6 Histology

After recording, pups are overdosed with sodium pentobarbital (1.5 mg/g i.p.) or a ketamine/xylazine cocktail (90:10; .002 mL/g i.p.) and transcardially perfused with phosphate-buffered saline followed by 4% paraformaldehyde. The recording site is visualized on 80 μ m sections under a microscope with fluorescent illumination at 5–10 \times magnification (Leica Microsystems, Buffalo Grove, IL). Recording site locations are subsequently determined after Nissl staining using a calibrated reticle. A photomicrograph of the CN and electrode placement in the interpositus nucleus is shown in Fig. 4. For unquestionable identification of the origin of any extracellular activity in the cerebellum that is not from a Purkinje cell, juxtacellular labeling is necessary (see Chap. 1 in this volume; [34]).

2.7 Pros and Cons of Head-Fix Recording in Relation to Testing Freely Moving Pups

The head-fix method has several advantages. First, because of the small size and uncalcified skulls of rodent pups, it is difficult to secure electrodes to the skull for chronic recording in freely moving subjects. Second, recordings using the head-fix method are

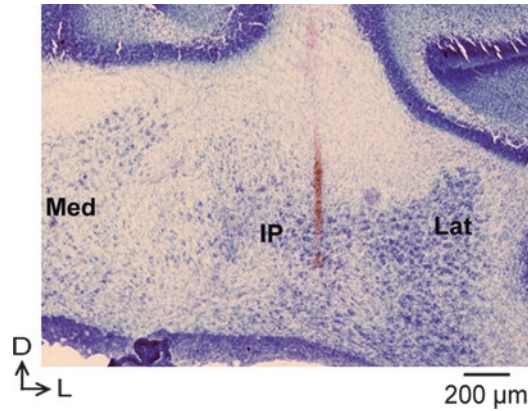


Fig. 4 Magnified Nissl-stained coronal section of the CN of a P12 rat. Red line indicates electrode location from identification of fluorescent Dil tracks in the same coronal sections. *IP* interpositus nucleus, *Lat* lateral nucleus, *Med* medial nucleus, *D* dorsal, *L* lateral

relatively free of movement artifact. Third, the head-fix method affords the experimenter the ability to adjust electrode location until the expected extracellular activity is observed and facilitates extracellular recording in combination with other manipulations, such as pharmacological inactivation [35–37]. This method is also well suited to the use of controlled peripheral stimulation in conjunction with extracellular recording (e.g., [38, 39]). Finally, for methods like two-photon imaging [40] and voltage-sensitive dye imaging [41, 42], there are no good alternatives to the head-fix method for studying brain activity in unanesthetized pups. In adult mice and rats, the head-fix method has similarly been used in conjunction with a number of different paradigms, including eyeblink conditioning ([43]; see Chap. 10 of this volume for a detailed description).

Although the head-fix method provides an environment that allows the pup to sleep comfortably, it is not ideal for pups to be separated from their mother and littermates—including the tactile, olfactory, and thermal features of the normal habitat [44]—for an extended period of time. Recently, a study examining cerebral cortical activity in head-fixed infant rats used a paradigm that included the presence of a littermate in contact with the head-fixed subject [45]. These and other modifications to the method can be developed to expand the range of questions that can be asked and resolve concerns about the artificiality of the testing procedure.

2.8 Pros and Cons of Recording Neural Activity in Unanesthetized Subjects

For those research questions in which behavior is not a priority, it may be preferable to use anesthetized subjects. However, given that anesthetics can substantially alter neural activity at the cellular and network levels, it is preferable—whenever possible—to use unanesthetized subjects. Indeed, as described

below, most of the difficulties of working with behaving animals, including infants, can be avoided by considering potential pitfalls in advance.

Unlike head-fixed adult subjects, infant subjects do not require days or weeks of habituation to the restraint; on the contrary, we observe regular sleep-wake cycles within an hour or two of surgery. When head-fixed pups exhibit signs of distress, it is expressed in the form of pronounced and protracted limb movements and audible vocalizations. To resolve the problem, check to make sure that the head and neck are comfortably positioned in relation to the body and to the platform. Also, there are a number of issues to consider when testing pups after prolonged separation from the nest. Specifically, before P10, urogenital stimulation is required for micturition and defecation [46], and a pup sometimes will exhibit distress until it is voided by the experimenter (using a cotton-tipped applicator applied to the anogenital region). If a pup exhibits struggling movements or is vocalizing audibly for any extended period of time, temperature and humidity should be checked to ensure that the pup is neither too cold nor too hot and that the air is not too dry.

Mechanical vibration, including vibration resulting from body movements, can lead to artifacts in the electrophysiological recordings. EMG electrodes that are loose and dangling from the pup can result in noisy signals; securing the wires to a stable platform with tape usually resolves this problem. For a variety of reasons, including the proximity of the electrode to the neck and shoulder, cerebellar and hindbrain extracellular recordings are particularly prone to movement artifact. The attachment of the nuchal ligament and musculature to the occipital bone can be one source of movement artifact, especially in older pups. Therefore, to minimize movement artifact, an additional surgical step is to detach the nuchal ligament from its anchor point to the skull. This can be done via blunt dissection with forceps or scissor or by cauterizing at the attachment points. If movement artifact is still a problem, the occipital bone can be hardened with Vetbond.

Using head restraint with awake, behaving pups—especially at older ages—requires more diligence than with anesthetized preparations. Importantly, the second postnatal week is a time of substantial functional change in the auditory and visual systems, with implications for behavior [47–49]. For example, noise and lights that are undetectable during the first postnatal week can easily arouse a P9 mouse or a P12 rat. Lastly, the testing of tactile or proprioceptive responses becomes more difficult with age: Stimulation paradigms that are effective in young rat pups can cause profound arousal at P12.

3 Analyzing Extracellular Activity and Behavior

3.1 Recording from Purkinje Cells

As with adult rodents, infant Purkinje cell activity can be identified by the presence of complex and simple spikes. In infant rodents, however, complex spikes are unique in that they exhibit a neurophysiological signature reflective of the stage of climbing fiber synapse development [12, 17, 26] and Purkinje cell maturation [7]. Specifically, during the first 2 postnatal weeks, complex spikes present as multi-spike bursts of action potentials with inter-spike intervals of 10–50 ms depending on the age of the pup [12, 17, 50, 51]. Also, due to the multiple innervations of climbing fibers, complex spike firing rates may actually be higher in infants than in adults [26].

Because of these developmental differences in the characteristics of complex spikes, it is necessary to use an age-appropriate method for segregating complex and simple spikes. For both mouse and rat pups at P9 and younger, inter-spike interval alone can be used to identify a complex spike. Figure 5a shows representative inter-spike intervals for unit activity recorded from Purkinje cells in rats at P4, P8, and P12. Using frequency distributions of inter-spike intervals, we determined that inter-spike intervals ≤ 20 ms captured complex spike activity at P4 and inter-spike intervals ≤ 15 ms captured complex spike activity at P8 (Fig. 5b) [51]. On the basis of these inter-spike intervals and using a script implemented in Spike2 software (Cambridge Electronic Design, Cambridge, UK), complex spike bursts of two or more action potentials can be extracted from the overall unit activity and marked as single events. The remaining neural activity is designated as simple spike activity. At these ages, the firing rates for simple spikes are low in relation to adults (Table 2) [16].

By P12, complex spikes are more adult-like in form, although still variable [12, 17, 26]. Therefore, a spike sorting algorithm or template matching protocol must be used. In adults, investigators employ a number of different protocols to identify complex spikes (see [26] and [29] for slightly different examples). We sort spikes using the standard template matching algorithm in Spike2. Using a 3–5 ms window to extract each template, we can identify individual units. Once we have identified unit templates, we use the overdraw function in Spike2 to visualize the waveforms. Using a second threshold ($\geq 2:1$ signal-to-noise ratio), we identify subsequent depolarizations and visually verify that those depolarizations are characteristics of a complex spike (Fig. 5c). Importantly, over this 2-week period of development, the number of action potentials or components comprising complex spikes increases, while the intervals between adjacent components shorten. At the same time, simple spike firing rates increase (Fig. 5d) [12].

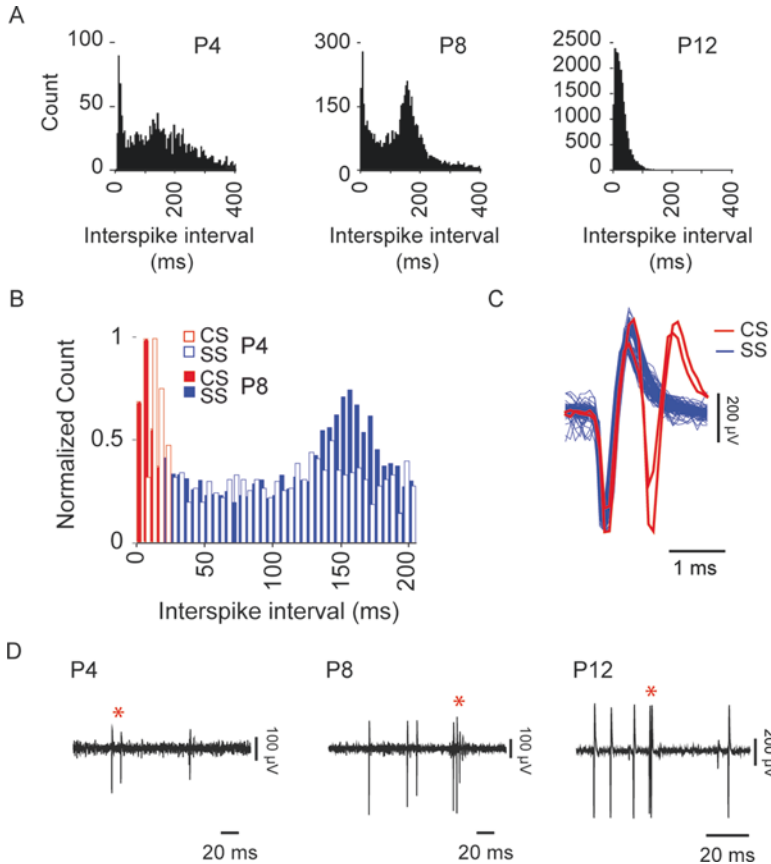


Fig. 5 Determining Purkinje cell activity in the postnatal rat. (a) Inter-spike interval histograms for Purkinje cells at P4, P8, and P12. Note, at P4 and P8, that the inter-spike intervals suggest two patterns of neural activity—one fast (i.e., < 50 ms) and the other slower (~ 100 – 200 ms). (b) Determination of complex spike (CS) and simple spike (SS) activity for P4 and P8 rats. In P4 rats, CSs are defined from action potentials with inter-spike intervals ≤ 20 ms. At P8, inter-spike intervals are faster and CSs are defined from action potentials with inter-spike intervals ≤ 15 ms. All remaining activity is classified as SSs. (c) Determination of CS and SS activity in P12 rats. By P12, CS more closely resembles the adult form. Using a larger window to extract templates, CSs can be identified using the overdraw method in Spike2 to visualize templates with multiple depolarizations. (d) Representative multiunit activity at P4, P8, and P12 illustrating the maturation of the CS and the increase in SS activity

3.2 Recording from Other Cell Types in the Cerebellar Cortex and Cerebellar Nuclei

Purkinje cell activity during postnatal development is easily identified by high-amplitude action potentials and the presence of complex and simple spikes. The neural activity of the other cell types within the cerebellar cortex and CN, however, is harder to identify without utilizing methodologies such as juxtacellular labeling (see Chap. 1 of this volume; [34, 52]). Based on histology and patterns of extracellular activity, however, it is possible to ascertain the cell type with reasonable certainty (Fig. 6a) [34]. Furthermore, during postnatal development, certain cell types may be ruled out at certain ages (i.e., basket cells are not functional at P4) [3, 4, 8, 9].

Table 2
Mean firing rate of Purkinje cells and neurons in the interpositus nucleus during early postnatal development

	Age	Mean firing rate (Hz)
Complex spikes	P4	0.19 ± 0.0
	P8	0.64 ± 0.1
	P12	1.66 ± 0.2
Simple spikes	P4	1.87 ± 0.3
	P8	4.56 ± 0.5
	P12	11.84 ± 1.6
Interpositus nucleus	P8	3.09 ± 0.4
	P12	15.44 ± 2.6

P postnatal day. Means ± SEM

Consistent with anatomical and neurophysiological assessments of the development of the cerebellar cortex [3, 4, 8, 9], we have recorded non-Purkinje cell activity at P8 and, more commonly, at P12. Figure 6b (left) shows three channels of multiunit activity (MUA) recorded from adjacent sites within the cerebellar cortex of a P8 rat (see color coding in Fig. 6a); the corresponding inter-spike interval distributions are shown on the right. The MUA on channel 7 exhibited a typical Purkinje cell activity profile with high-amplitude action potentials and a relatively tonic firing rate (Fig. 6b, green); moreover, inter-spike intervals show the double peak typically seen at this age [16, 51]. In contrast, the MUA on channels 6 and 8 (Fig. 6b, blue and pink, respectively) only increased when the Purkinje cell was silent. These electrode sites (NeuroNexus model, A1x16-Poly2-5 mm-50s-177; site diameter = 15 μm) were situated just above and below (~43.3 μm) and lateral (± 25 μm) to the site where Purkinje cell activity was detected. This pattern of activity and inter-spike interval distributions (Fig. 6b, right) are consistent with basket or Golgi cells [34, 51].

In older infants, the IGL is large enough for the electrode to be contained entirely within it. The photomicrograph in Fig. 6c shows the IGL of cortical layers IV/V in a P14 mouse: It is apparent that all recording sites of the electrode were contained deep within the IGL. Furthermore, for one neuron, an exceptionally fast firing rate was observed. The raw MUA activity is presented below the histology image and enlarged at the right to show the bursting properties of this cell (Fig. 6c, bottom). This activity is very similar to what has been observed in extracellular recordings of granule cells in adult rabbits and mice [53].

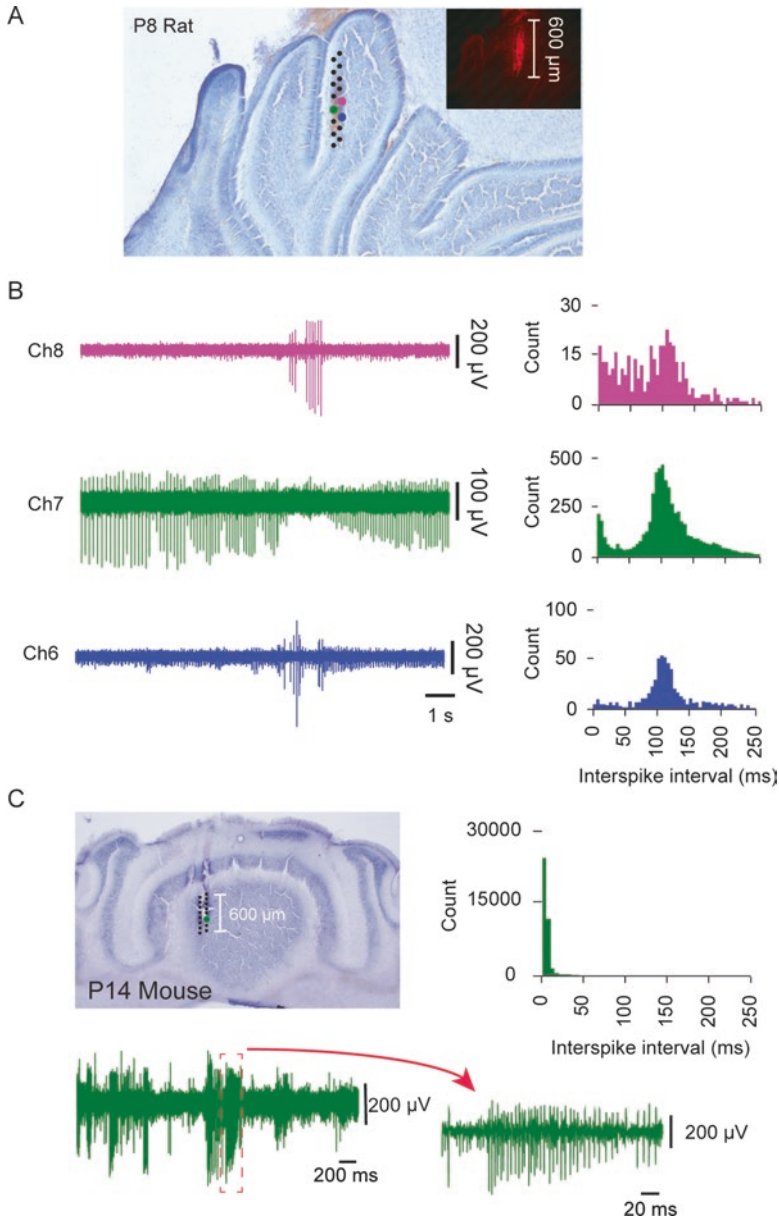


Fig. 6 Classifying cerebellar unit activity using inter-spike interval. **(a)** Nissl-stained, coronal section from a P8 rat showing electrode placement in Crus 1 of the cerebellar cortex. Filled circles illustrate electrode site locations (not drawn to scale). **Inset**, Fluorescent micrograph showing Dil fluorescence used for histological verification. **(b) Left**, Three channels of multiunit activity corresponding to the colored circles in **(a)**. All sites were situated in closest proximity to the Purkinje cell layer. **Right**, Inter-spike interval histograms for the single unit activity from each of the MUA channels. Patterning and rate differ across the channels with channel 7 (Ch7) exhibiting the inter-spike interval pattern of a P8 Purkinje cell; the sites for channels 6 and 8 (Ch6 and Ch8) are immediately below (relative to the Purkinje cell layer) the site for Ch7 suggestive of cortical inhibitory neurons such as basket or Golgi cells. **(c) Upper left**, Nissl-stained, coronal section from a P14 mouse showing electrode placement in the internal granular layer of layers 4 and 5 of the cerebellar cortex. Green circle indicates approximate position of electrode site. **Upper right**, The inter-spike interval histogram on the right shows that the inter-spike interval was very brief. **Lower left**, The raw MUA record illustrates that the high firing rate occurs in bursts and is expanded, **lower right**, to show a brief period of rapid bursting in this unit, similar to what has been seen in granule cell recordings in the adult mouse and rabbit [53]

The extracellular activity of the cerebellar nuclei (CN) during motor learning in adult rodents has been well studied [54–56]. However, surprisingly little is known about CN activity across the early postnatal period [9, 10, 19]. Perhaps the best developmental research on CN activity in developing rats has focused on eyeblink conditioning during the third postnatal week [57]. In that work, extracellular activity in the interpositus nucleus exhibited developmental changes in activity that relates to the expression of conditioned responses in a way that is consistent with granule cell migration and cerebellar circuit formation.

Recently, we recorded extracellular activity in the interpositus nucleus in rats at P8 and P12. Similar to Purkinje cell activity [51], there was a substantial increase in firing rate between P8 and P12 (Table 2) [36]. Consistent with *in vivo* recordings in adults, extracellular activity in the developing CN exhibits heterogeneity in firing rate, consistent with the heterogeneity of cell types within the nuclei [52]. We also found that inactivation of the interpositus, using the GABA_A receptor agonist muscimol, reduced spontaneous activity in the red nucleus—which receives a major interpositus projection—by approximately 50% at both P8 and P12 [36]. Importantly, this finding demonstrates functional connectivity of the cerebellum with the brainstem very early in the postnatal period.

3.3 Cerebellar Activity and Behavior

In his seminal work in the 1970s on cerebellar anatomy in perinatal rats, Altman showed how the expression of skilled motor behavior occurs in lockstep with cerebellar development [1, 5, 58]. In the intervening years, much has been learned about the molecular mechanisms involved in cerebellar development [20, 21]. In addition, evidence has begun to accumulate that activity-dependent processes are also involved [21, 25]. We have sought to identify those mechanisms and how they might contribute to somatotopic organization within the cerebellar circuit [36, 50, 51].

During the first postnatal week in rats, active (or REM) sleep is the predominant behavioral state [59, 60]. The hallmark of active sleep is the muscle atonia accompanied by myoclonic twitches of skeletal muscles, resulting in hundreds of thousands of discrete jerky movements of the limbs and whiskers each day [61]. Accordingly, twitching is the predominant motor behavior of the early postnatal period. Importantly, twitch-related sensory feedback influences spinal circuit formation [62] and triggers substantial neural activity in many brain areas, including the thalamus, hippocampus, and cerebral cortex [39, 42, 63–65]. The same holds true for the cerebellum: Both Purkinje cell and interpositus activity exhibit strong sleep dependency, with more neural activity occurring during active sleep than wakefulness. Furthermore, feedback from twitches triggers increased cerebellar activity [36, 50, 51]. These observations are building a case for the importance of sleep in early development, as well as for the consideration

of twitching as a self-generated form of spontaneous activity that contributes to the activity-dependent development of sensorimotor systems [36–39, 50, 51, 66].

To examine sleep-related cerebellar activity, we quantify behavioral state using EMG and behavioral scoring. First, the EMG record is rectified and smoothed ($\tau = 0.001$ s). The mean EMG signal for periods of atonia (sleep) and high muscle tone (wake) is calculated from five representative 1 s EMG segments. The midpoint between these two values is used as a threshold for identifying sleep and wake. Once the threshold is determined, the experimental session can be coded using the EMG signal to identify periods of sleep and wake, with behavioral observation used to confirm these designations. Sleep can be further divided into periods of quiet sleep (low tone/tonia with behavioral quiescence) and active sleep (tonia with myoclonic twitches) [50, 51]. Figure 7a shows a representative Purkinje cell MUA and EMG activity from a P12 rat. The record begins with the pup in active sleep as evidenced by both nuchal and hind limb atonia. When the rat pup awakens (gray box) and moves vigorously, the neural activity decreases. Then, when the pup stops moving and becomes quiet again, the neural activity returns.

Similar to studies examining cerebellar activity during learning, perievent histograms provide a straightforward way to assess the neural response to twitches. First, we identify individual twitches as discrete EMG events with amplitudes exceeding at least three times the mean EMG level during atonia [50, 51]. With twitches converted into discrete events, it is easy to quantify the neural activity in the vicinity of a twitch; in Fig. 7b, complex spike activity increases substantially within 100 ms of twitching. The same approach can be taken for examining the effects of exafferent stimuli on cerebellar activity (Fig. 7c). In Fig. 7c, interpositus activity increases substantially after ipsilateral forelimb stimulation. Twitch-reafference and exafferent stimulation of the limbs and face can be used to investigate somatotopic organization in the developing cerebellum.

4 Conclusions: New Approaches to Recording and Analyzing Extracellular Activity

The last decade has seen a profound increase in new molecular, neurophysiological, and neuroimaging methods that are improving our ability to observe and manipulate (e.g., optogenetics) neural activity on biologically relevant timescales [43, 52]. For example, the use of transgenic lines with conditional expression of GCaMP3 has been used in infant mice with two-photon imaging to examine neural activity in the developing visual system [67]. Furthermore, mouse lines with Cre-dependent, cell-specific expression of opsins makes it possible to use optogenetic approaches at the earliest

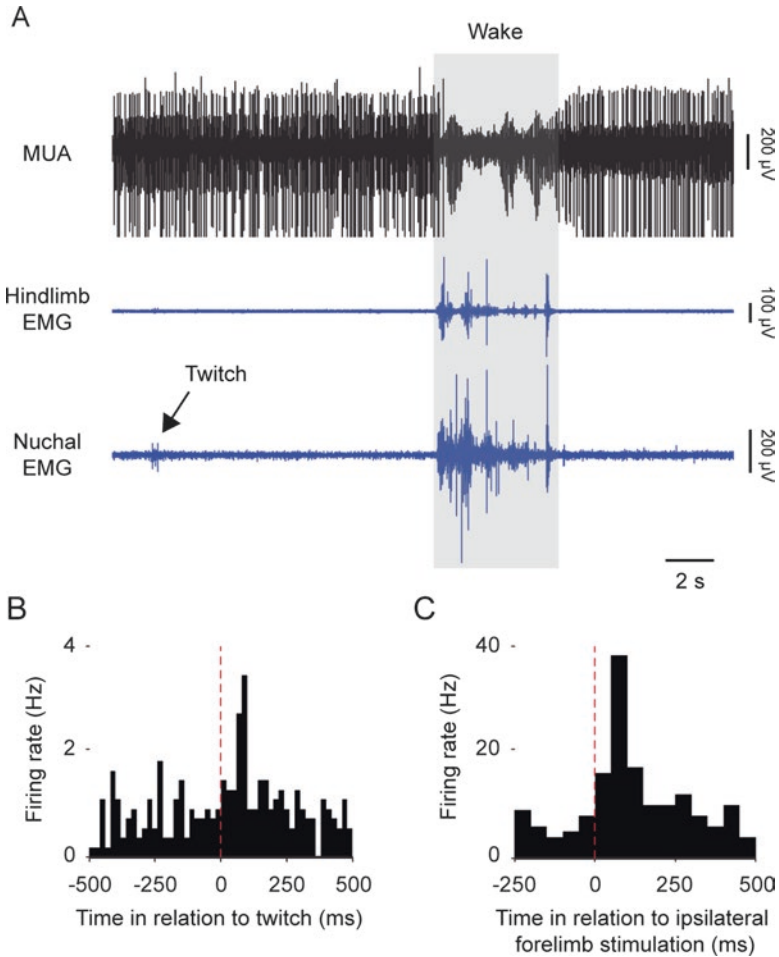


Fig. 7 Cerebellar activity and behavior in the postnatal rat. (a) Multiunit activity (MUA) and EMG activity from the ipsilateral hind limb and nuchal muscles for a representative P12 rat exhibiting state-dependent neural activity. The MUA exhibits a tonic, rapid rate of firing during active sleep (AS). However, when the pup wakes up and moves around the high amplitude unit, activity ceases. When the animal again becomes quiet and stops moving, the neural activity resumes. (b) Twitch-triggered event correlation for complex spike activity in a P8 rat. Approximately 60–80 ms following a twitch in the nuchal muscle complex spike activity increases. (c) Event correlation of CN activity recorded from the interpositus nucleus of a P12 rat in response to a forelimb stimulation. Over 18 stimulations, an increase in activity is observed 50–100 ms following the stimulation

postnatal ages [68]. These are just two examples of novel approaches for studying activity in the developing cerebellum using the head-fix method.

The head-fix method can also be modified for implementation in numerous testing environments. To date, no studies have used the head-fix method to look at goal-directed movements and extracellular cerebellar activity in infant rodents. In infant rats, this could provide a means to assess the effects of early motor training on cerebellar activity and vice versa. For example, an adaptation of

the cylindrical treadmill from the adult mouse head-fix preparation ([43]; see Chap. 10 of this volume) could provide a measure of cerebellar responses to practiced or novel wake movements in infant rats and mice. We know from previous work that direct stimulation of the pontine nuclei in P12 rats is a potent conditioned stimulus, resulting in a conditioned eyeblink response [69]. This result clarified that the previously reported absence of motor learning is a result of developmental immaturity of sensory pathways and not immaturity of plasticity mechanisms in cerebellar circuits [5]. Given that the red nucleus receives inputs from the CN as early as P8 and that inactivation of the interpositus nucleus significantly reduces red nucleus extracellular activity, it appears that the CN exerts excitatory control over premotor areas at very young ages [36]. Perhaps the incorporation of age-appropriate sensory stimuli (i.e., vibration; [70, 71]) and/or age-appropriate motor tasks [58] would allow for the study of learning-related cerebellar activity at earlier ages than previously thought possible.

Importantly, extracellular activity in the infant rat cerebellum shows changes in patterning, timing, variety, and quantity of activity during the first 2 postnatal weeks in rats [36, 50, 51]. This corresponds to a period of rapid and dramatic development in cerebellar circuitry. Two important patterns observed during this period are the sleep- and twitch-dependent activities of the cerebellar cortex and CN, which suggest this may be a sensitive period for activity-dependent development [36, 50, 51]. Although the rodent cerebellum continues to develop beyond the first postnatal month, many critical developmental changes occur in the first 2 postnatal weeks; therefore, if these changes depend on activity-dependent processes, it would make cerebellar development susceptible to environmental factors that might affect sleep or sleep quality early in development [51]. It remains to be determined how subtle and variable deficits in cerebellar development translate into neurobehavioral disorders [28]. Therefore, a comprehensive understanding of early postnatal cerebellar activity and the susceptibility of that activity to environmental insult remains an important line of research that could benefit greatly from the head-fix method.

References

1. Addison WHF (1911) The development of the Purkinje cells and of the cortical layers in the cerebellum of the albino rat. *J Comp Neurol* 21:459–486
2. Altman J (1972) Postnatal development of the cerebellar cortex in the rat I. The external germinal layer and the transitional molecular layer. *J Comp Neurol* 145:353–398
3. Altman J (1972) Postnatal development of the cerebellar cortex in the rat II. Phases in the maturation of Purkinje cells and of the molecular layer. *J Comp Neurol* 145:399–464
4. Altman J (1972) Postnatal development of the cerebellar cortex in the rat III. Maturation of the components of the granular layer. *J Comp Neurol* 145:465–514

5. Freeman JH (2014) The ontogeny of associative cerebellar learning. In: Mauk MD (ed) International review of neurobiology: Cerebellar conditioning and learning. Elsevier, Oxford, pp 53–71
6. Hashimoto K et al (2009) Translocation of a “winner” climbing fiber to the Purkinje cell dendrite and subsequent elimination of “losers” from the soma in developing cerebellum. *Neuron* 63:106–118
7. McKay BE, Turner RW (2005) Physiological and morphological development of the rat. *J Physiol* 567:829–850
8. Shimono T, Nosaka S, Sasaki K (1976) Electrophysiological study on the postnatal development of neuronal mechanisms in the rat cerebellar cortex. *Brain Res* 108:279–294
9. Crepel F (1974) Excitatory and inhibitory processes acting upon cerebellar Purkinje cells during maturation in the rat; Influence of hypothyroidism. *Exp Brain Res* 20:403–420
10. Gardette R et al (1985) Electrophysiological studies on the postnatal development of intracerebellar nuclei neurons in rat cerebellar slices maintained in vitro. I. Postsynaptic potentials. *Dev Brain Res* 19:47–55
11. Kalinovskiy A et al (2011) Development of axon-target specificity of ponto-cerebellar afferents. *PLoS Biol.* <https://doi.org/10.1371/journal.pbio.1001013>
12. Crepel F (1971) Maturation of climbing fiber responses in the rat. *Brain Res* 35:272–276
13. Crepel F, Mariani J, Delhaye-Bouchaud N (1976) Evidence for a multiple innervation of Purkinje cells by climbing fibers in the immature rat cerebellum. *J Neurobiol* 7:567–578
14. Hashimoto K, Kano M (2005) Postnatal development and synapse elimination of climbing fiber to Purkinje cell projection in the cerebellum. *Neurosci Res* 53:221–228
15. Kuwako K-I et al (2014) Cadherin-7 regulates mossy fiber connectivity in the cerebellum. *Cell Rep* 9:311–323
16. Woodward DJ, Hoffer BJ, Lapham LW (1969) Postnatal development of electrical and enzyme histochemical activity in Purkinje cells. *Exp Neurol* 23:120–139
17. Puro DG, Woodward DJ (1977) Maturation of evoked climbing fiber input to rat cerebellar Purkinje cells (I.). *Exp Brain Res* 28:85–100
18. Puro DG, Woodward DJ (1977) Maturation of evoked mossy fiber input to rat cerebellar Purkinje cells (II). *Exp Brain Res* 28:427–441
19. Gardette R et al (1985) Electrophysiological studies on the postnatal development of intracerebellar nuclei neurons in rat cerebellar slices maintained in vitro. II. Membrane conductances. *Dev Brain Res* 20:97–106
20. Sillitoe RV, Joyner AL (2007) Morphology, molecular codes, and circuitry produce the three-dimensional complexity of the cerebellum. *Annu Rev Cell Dev Biol* 23:549–577
21. Wang VY, Zoghbi HY (2001) Genetic regulation of cerebellar development. *Nat Rev Neurosci* 2:484–491
22. Hashimoto K, Kano M (2013) Synapse elimination in the developing cerebellum. *Cell Mol Life Sci* 70:4667–4680
23. Bosman LWJ et al (2008) Homosynaptic long-term synaptic potentiation of the “winner” climbing fiber synapse in developing Purkinje cells. *J Neurosci* 28:798–807
24. Kakizawa S et al (2000) Critical period for activity-dependent synapse elimination in developing cerebellum. *J Neurosci* 20:4954–4951
25. Kano M, Hashimoto K (2012) Activity-dependent maturation of climbing fiber to Purkinje cell synapses during postnatal cerebellar development. *Cerebellum* 11:449–450
26. Lorenzetto E et al (2009) Genetic perturbation of postsynaptic activity regulates synapse elimination in developing cerebellum. *PNAS* 106:16475–16480
27. Watanabe M, Kano M (2011) Climbing fiber synapse elimination in cerebellar Purkinje cells. *Eur J Neurosci* 34:1697–1710
28. Wang SS-H, Kloth AD, Badura A (2014) The cerebellum, sensitive periods, and autism. *Neuron* 83:518–532
29. Arancillo M et al (2015) In vivo analysis of Purkinje cell firing properties during postnatal mouse development. *J Neurophysiol* 113:578–591
30. Ito M (2008) Control of mental activities by internal models in the cerebellum. *Nat Rev Neurosci* 9:304–313
31. Shevelkin AV, Ihenatu C, Pletnikov MV (2014) Pre-clinical models of neurodevelopmental disorders: Focus on the cerebellum. *Rev Neurosci* 25:177–197
32. Blumberg MS et al (2015) A valuable and promising method for recording brain activity in behaving newborn rodents. *Dev Psychobiol* 57:506–517
33. Seelke AMH, Blumberg MS (2005) The microstructure of active and quiet sleep as cortical delta activity emerges in infant rats. *Sleep* 31:691–699
34. Ruigrok TJH, Hensbroek RA, Simpson RI (2011) Spontaneous activity signatures of morphologically identified interneurons in the vestibulocerebellum. *J Neurosci* 31:712–724

35. Del Rio-Bermudez C, Sokoloff G, Blumberg MS (2015) Sensorimotor processing in the newborn rat red nucleus during active sleep. *J Neurosci* 35:8322–8332
36. Del Rio-Bermudez C et al (2016) Spontaneous activity and functional connectivity in the developing cerebellorubral system. *J Neurophysiol* 116:1316–1327
37. Tiriác A, Blumberg MS (2016) Gating of reafference in the external cuneate nucleus during self-generated movements in wake but not sleep. *Elife*. <https://doi.org/10.7554/eLife.18749>.
38. An S, Kilb W, Luhmann HJ (2014) Sensory-evoked and spontaneous gamma and spindle bursts in neonatal rat motor cortex. *J Neurosci* 34:10870–10883
39. Tiriác A, Rio-Bermudez CD, Blumberg MS (2014) Self-generated movements with “unexpected” sensory consequences. *Curr Biol* 24:2136–2141
40. Kummer M et al (2016) Column-like CA2+ clusters in the mouse neonatal neocortex revealed by three-dimensional two-photon CA2+ imaging in vivo. *Neuroimage* 138:64–75
41. Luhmann HJ (2016) Review of imaging network activities in developing rodent cerebral cortex in vivo. *Neurophoton*. <https://doi.org/10.1117/1.NPh.4.3.031202>
42. Tiriác A, Uitermarkt BD, Fanning AS, Sokoloff G, Blumberg MS (2012) Rapid whisker movements in sleeping newborn rats. *Curr Biol* 22:2075–2080
43. Heiney SA et al (2014) Cerebellar-dependent expression of motor learning during eyeblink conditioning in head-fixed mice. *J Neurosci* 34:14845–14853
44. Alberts JR, Cramer CP (1988) Ecology and experience: Sources of means and meaning of developmental change. In: Blass EM (ed) *Developmental psychobiology and behavioral ecology*. Springer, New York, pp 1–39
45. Akhmetshina D et al (2016) The nature of the sensory input to the neonatal rat barrel cortex. *J Neurosci* 36:9922–9932
46. Stelzner DJ (1971) The normal postnatal development of synaptic end-feet in the lumbosacral spinal cord and of responses in the hind limbs of the albino rat. *Exp Neurol* 31:331–357
47. Blatchley BJ, Cooper WA, Coleman JR (1987) Development of auditory brainstem response to tone pip stimuli in the rat. *Dev Brain Res* 32:75–84
48. Blumberg MS et al (2005) Dynamics of sleep-wake cyclicity in developing rats. *PNAS* 102:14860–14864
49. Routtenberg A, Strop M, Jerden J (1978) Response of the infant rat to light prior to eyelid opening: mediation by the superior colliculus. *Dev Psychobiol* 11:469–478
50. Sokoloff G, Uitermarkt BD, Blumberg MS (2015) REM sleep twitches rouse nascent cerebellar circuits: implications for sensorimotor development. *Dev Neurobiol* 75:1140–1153
51. Sokoloff G et al (2015) Twitch-related and rhythmic activation of the developing cerebellar cortex. *J Neurophysiol* 114:1746–1756
52. Canto CB, Witter L, De Zeeuw CI (2016) Whole-cell properties of cerebellar nuclei neurons in vivo. *PLoS One*. <https://doi.org/10.1371/journal.pone.0165887>
53. van Beugen BJ, Gao Z, Boele H-J, Hoebeek F, De Zeeuw CI (2013) High frequency burst firing of granule cells ensures transmission at the parallel to Purkinje cell synapse at the cost of temporal coding. *Front Neural Circuit*. <https://doi.org/10.3389/fncir.2013.00095>
54. Mauk MD (1997) Roles of cerebellar cortex and nuclei in motor learning: contradictions or clues? *Neuron* 18:343–346
55. Lee KH et al (2015) Circuit mechanisms underlying motor memory formation in the cerebellum. *Neuron* 86:529–540
56. Perciavalle V et al (2013) Consensus paper: current views on the role of cerebellar interpositus nucleus in movement control and emotion. *Cerebellum* 12:738–757
57. Freeman JH, Nicholson DA (2000) Developmental changes in eye-blink conditioning and neuronal activity in the cerebellar interpositus nucleus. *J Neurosci* 20:813–819
58. Altman J, Sudarshan K (1975) Postnatal development of locomotion in the laboratory rat. *Anim Behav* 23:896–920
59. Jouvet-Mounier D, Astic L, Lacote D (1969) Ontogenesis of the states of sleep in rat, cat, and guinea pig during the first postnatal month. *Dev Psychobiol* 2:216–239
60. Gramsbergen A, Schwartz P, Precht HFR (1970) The postnatal development of behavioral states in the rat. *Dev Psychobiol* 3:267–280
61. Blumberg MS, Marques HG, Iida F (2013) Twitching in sensorimotor development from sleeping rats to robots. *Curr Biol* 23:R532–R537
62. Petersson P et al (2003) Spontaneous muscle twitches during sleep guide spinal self-organization. *Nature* 424:72–75
63. Khazipov R et al (2004) Early motor activity drives spindle bursts in the developing somatosensory cortex. *Nature* 432:758–761

64. Mohns EJ, Blumberg MS (2008) Synchronous bursts of neuronal activity in the developing hippocampus: modulation by active sleep and association with emerging gamma and theta rhythms. *J Neurosci* 28:10134–10144
65. Mohns EJ, Blumberg MS (2010) Neocortical activation of the hippocampus during sleep in infant rats. *J Neurosci* 30:3438–3449
66. Roffwarg HP, Muzio JN, Dement WC (1966) Ontogenetic development of the human sleep-dream cycle. *Science* 152:604–619
67. Ackman JB, Burbridge TJ, Crair MC (2012) Retinal waves coordinate patterned activity throughout the developing visual system. *Nature* 490:219–225
68. Madisen L et al (2012) A toolbox of Cre-dependent optogenetic transgenic mice for light-induced activation and silencing. *Nat Neurosci* 15:793–802
69. Campolattaro MM, Freeman JH (2008) Eyeblink conditioning in 12-day-old rats using pontine stimulation as the conditioned stimulus. *PNAS* 105:8120–8123
70. Goldsberry ME, Elkin ME, Freeman JH (2014) Sensory system development influences the ontogeny of eyeblink conditioning. *Dev Psychobiol* 56:1244–1251
71. Goldsberry ME, Freeman JH (2016) Sensory system development influences the ontogeny of trace eyeblink conditioning. *Dev Psychobiol*. <https://doi.org/10.1002/dev.21468>